

Supporting information

Synthesis, Characterization of the Keggin type Ruthenium-Nitrido Derivative $[\text{PW}_{11}\text{O}_{39}\{\text{RuN}\}]^{4-}$ and Evidence of its Electrophilic Reactivity

Vanina Lahootun, Claire Besson, Richard Villanneau, Françoise Villain, Lise-Marie Chamoreau, Kamal Boubekeur, Sébastien Blanchard, René Thouvenot, Anna Proust*

EDX study of $\text{Cs}_4[\text{PW}_{11}\text{O}_{39}\{\text{RuN}\}]$ (TBA-1)

The formation of **Cs-1** was also investigated by energy dispersive X-ray spectroscopy (EDX). Indeed, this spectroscopy may be used as a quantitative analysis tool. The organometallic derivative $[\text{PW}_{11}\text{O}_{39}\{\text{Ru}(\text{H}_2\text{O})(p\text{-cymène})\}]^{5-}$ was used as a reference compound so as to study the ratio of the different metals in the analyzed POM. The data collected for the two samples are shown below (Figure 1). The superimposition of the two spectra shows that the intensities of the W and Ru peaks are exactly the same in both compounds. The intensity of these peaks being directly proportional to the concentration of the element being analyzed, these results suggest a W/Ru ratio equal to 11 as expected in **1**.

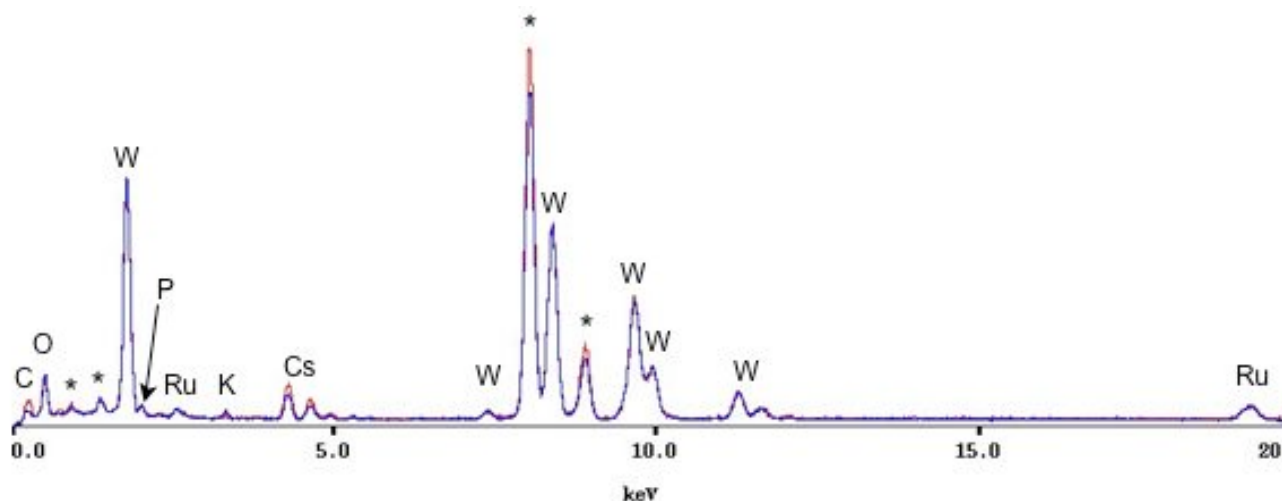


Figure 1: EDX spectra of $\text{Cs}_4[\text{PW}_{11}\text{O}_{39}\{\text{RuN}\}]$ (in red) and $\text{Cs}_{5-x}\text{K}_x[\text{PW}_{11}\text{O}_{39}\{\text{Ru}(\text{H}_2\text{O})(p\text{-cymène})\}]$ (in blue). (*: peaks due to the Cu cathode)

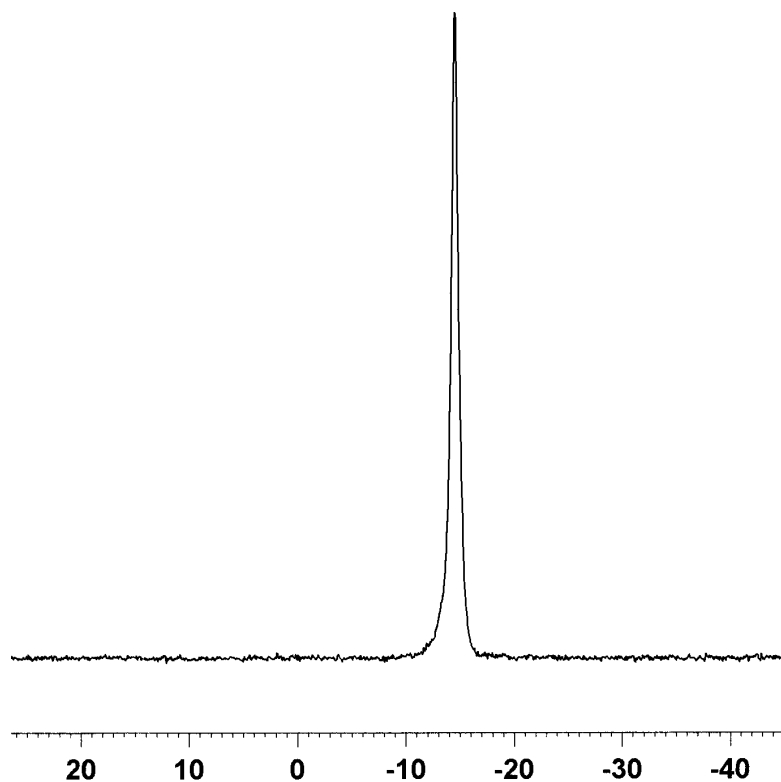


Figure 2: ^{31}P MAS NMR spectrum of $\text{Cs}_4[\text{PW}_{11}\text{O}_{39}\{\text{RuN}\}]$ (**Cs-1**) (recorded at room temperature on a Bruker Avance 400 spectrometer (9.4 T), at the Larmor frequency of 161.9 MHz with a 4 mm probe and a spinning speed of 8 kHz)

Strategy for the assignment of the ^{183}W NMR spectrum of $\text{TBA}_4[\text{PW}_{11}\text{O}_{39}\{\text{Ru}^{\text{VI}}\text{N}\}]$

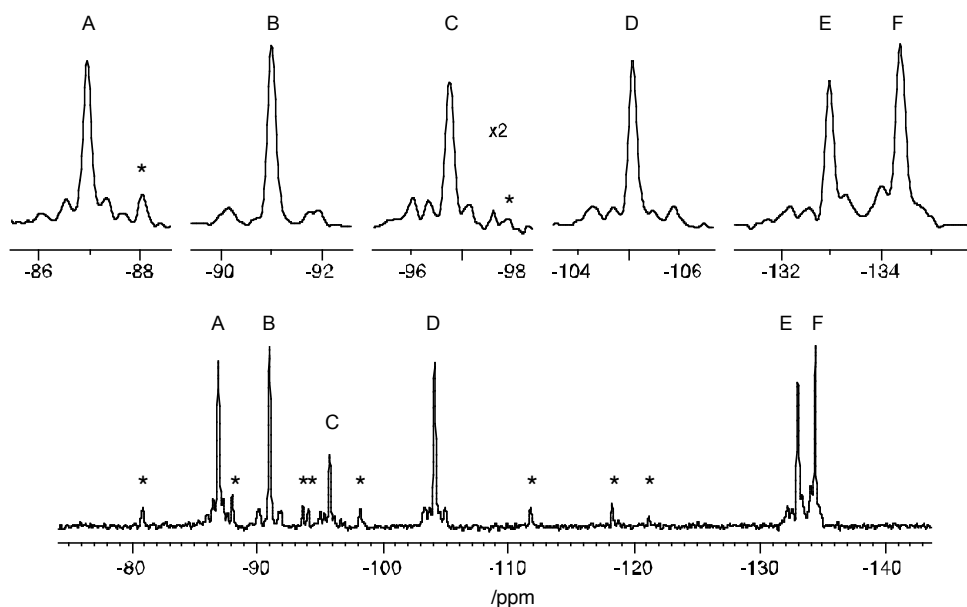


Figure 3 $^{183}\text{W}\{^{31}\text{P}\}$ NMR spectrum (12.5 MHz) of $\text{TBA}_4[\text{PW}_{11}\text{O}_{39}\{\text{Ru}^{\text{VI}}\text{N}\}]$ (**TBA-1**) ($1.2 \times 10^{-1} \text{ mol.L}^{-1}$ in DMF/D6-acetone ($T = 262 \text{ K}$)). Bottom: full spectrum; top: abscissa expansion of the individual resonances. The signal marked by * correspond to $[\text{H}_n\text{PW}_{11}\text{O}_{39}]^{(7-n)-}$ (ca 15%) and to $[\text{PW}_{12}\text{O}_{40}]^{3-}$ (ca 2%) impurities.

The connectivity matrix for a monosubstituted Keggin POM is recalled in Table 1 with numbering of the tungsten atoms given according to the IUPAC convention (see Figure 4).

Table 1 Theoretical tungsten-tungsten connectivity matrix for $[\alpha\text{-PW}_{11}\text{O}_{39}\text{ML}]^n$. Numbering of the atoms (see Figure 3) is given according to the IUPAC convention. Coupling constants are given off diagonal: e = edge (small) couplings, c = corner (large) couplings.

nucleus	2,3	4,9	5,8	6,7	10,12	11
2,3	δ		e	e		
4,9		δ	c		c	
5,8	e	c	δ	e	c	
6,7	e		e	δ		c
10,12		c	c		δ	e
11				c	e	δ

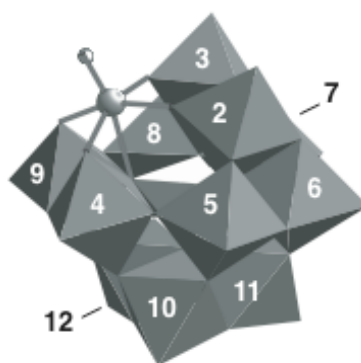


Figure 4. Postulated structure of $[\text{PW}_{11}\text{O}_{39}\{\text{Ru}^{\text{VI}}\text{N}\}]^4$ with W labels according to IUPAC convention.

The signal C with intensity 1 (-95.7 ppm) is immediately attributed to W11, in the plane of symmetry of **1**; for the five other resonances, unambiguous assignment requires determination of the W-W connectivity, either by correlation spectroscopy or by measurement of the W-W coupling constants. After resolution enhancement, (Figure 3, top) these satellites

become baseline-resolved from the central signal, which allows to measure the $^2J_{W-W}$ coupling constants. Unfortunately, only two different J values, namely ca 10 Hz ("edge" coupling), and ca 20 Hz ("corner" coupling), are observed and this does not permit to deduce the W-W connectivity. In that case, discrimination between the different tungsten nuclei could be done by the number and the type of coupling partners of each W, *i.e.* by relative integration of the satellite patterns. (reference48 in the text) Hence the three resonances A (-86.9), B (-91.0) and D (-104.1) are consistently assigned to W6 \equiv W7 (two edge, one corner), W4 \equiv W9 (no edge, two corner) and W10 \equiv W12 (one edge, two corner), respectively. This assignment agrees with the second-order AB system observed for the external satellites of resonances A and C, as well as for the resonance B. Partial overlap of the satellites of the signals around -130 ppm makes more difficult their assignment; nevertheless observation of a satellite at ca 10 Hz on the left side of E (-133.0) leads to assign this signal to W5 \equiv W8, while F (-134.4) without any corner coupling corresponds therefore to W2 \equiv W3.

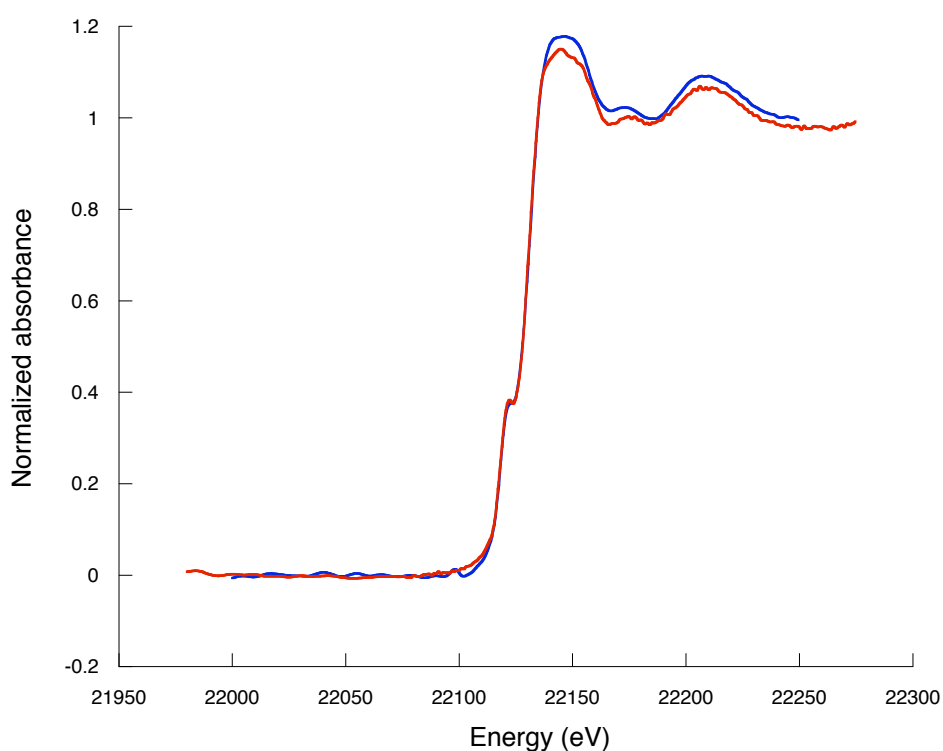


Figure 5: Ru- K edge XANES spectra of $\text{Cs}_4[\text{PW}_{11}\text{O}_{39}\{\text{RuN}\}]$ (**Cs-1**) (in red) and $\text{TBA}_4[\text{PW}_{11}\text{O}_{39}\{\text{RuN}\}]$ (**TBA-1**) (in blue)

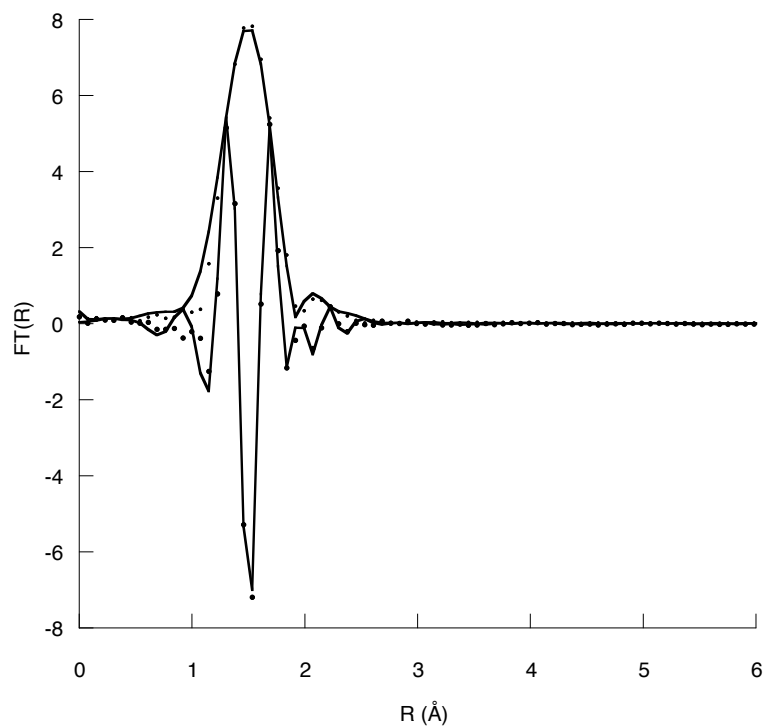


Figure 6: Modulus and imaginary part of the Fourier Transform of $\text{TBA}_4[\text{PW}_{11}\text{O}_{39}\{\text{RuN}\}]$ (**TBA-1**) filtered between 1 and 2.5 Å (first coordination sphere): experimental data in dotted line, simulated data in straight line

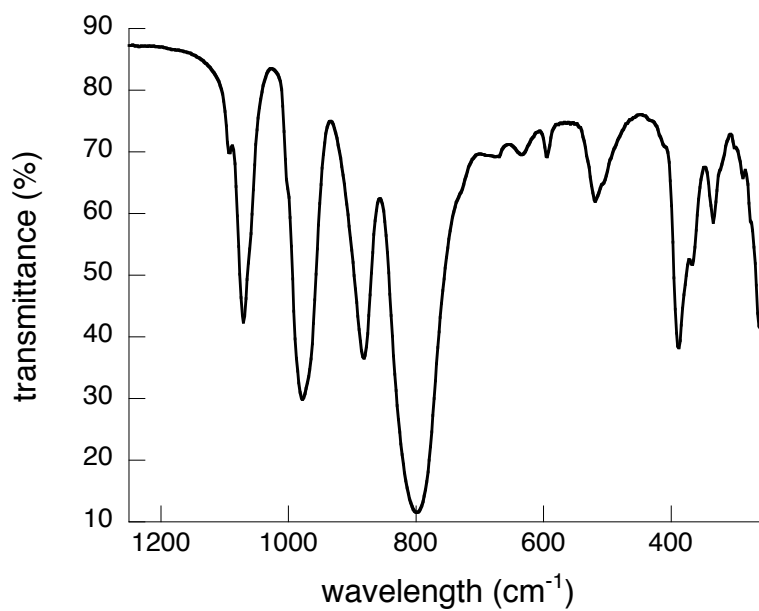


Figure 7: IR spectrum of $\text{Cs}_4[\text{PW}_{11}\text{O}_{39}\{\text{RuN}\}]$ (**Cs-1**)

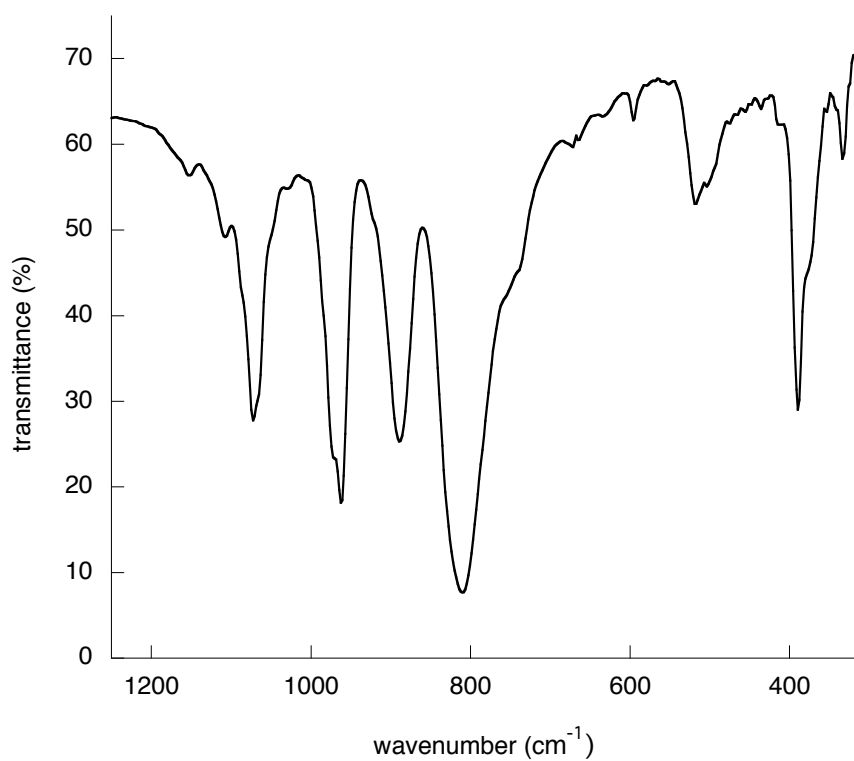


Figure 8: IR spectrum of $\text{TBA}_4[\text{PW}_{11}\text{O}_{39}\{\text{RuN}\}]$ (TBA-1)

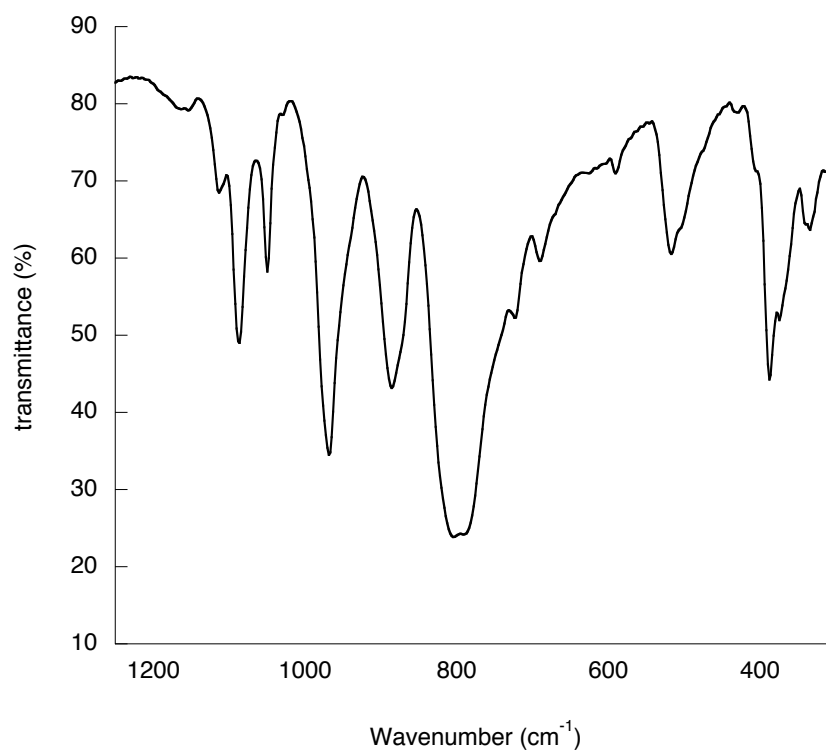


Figure 9: IR spectrum of $\text{TBA}_3[\text{PW}_{11}\text{O}_{39}\{\text{RuNPPH}_3\}]$ (2)

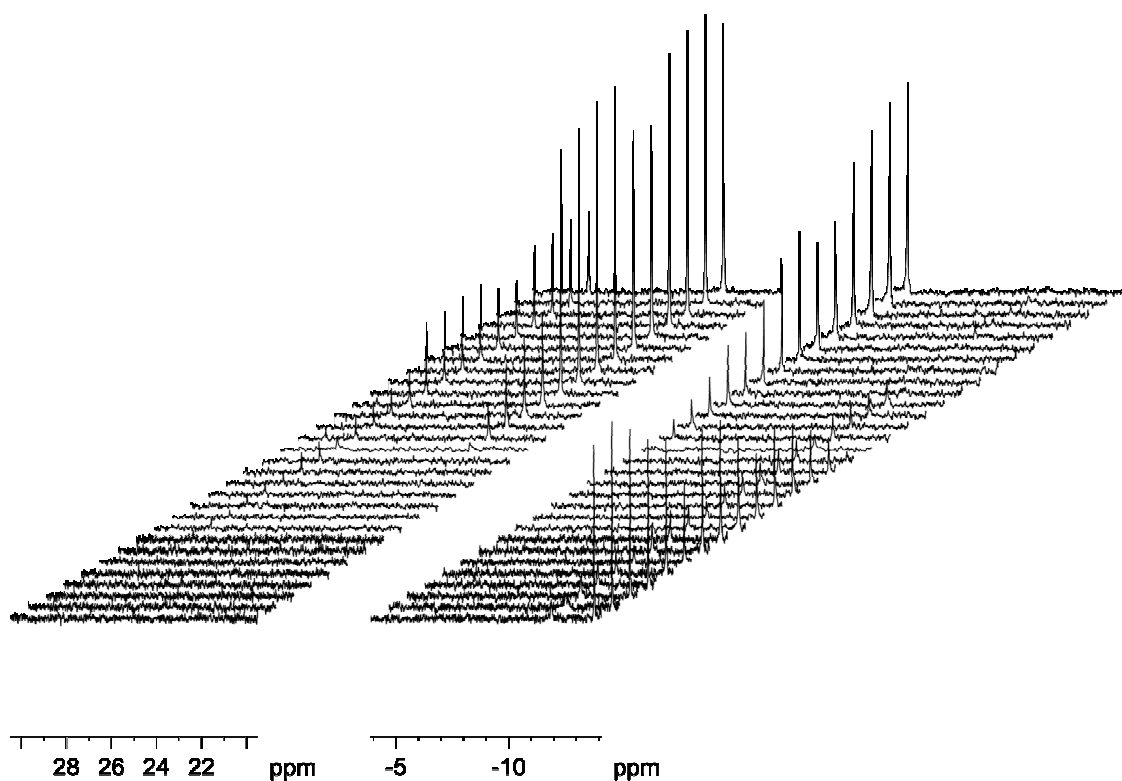


Figure 10: Evolution of the ^{31}P NMR spectrum of $\text{TBA}_4[\text{PW}_{11}\text{O}_{39}\{\text{Ru}^{\text{VI}}\text{N}\}]$ (**TBA-1**) in $\text{CH}_3\text{CN}/\text{CD}_3\text{CN}$ (3:1) in the presence of increasing amounts (from 0.1 (bottom) to 2.9 (top) equivalents) of PPh_3 in the range +30 -15 ppm (for the full spectra see manuscript)

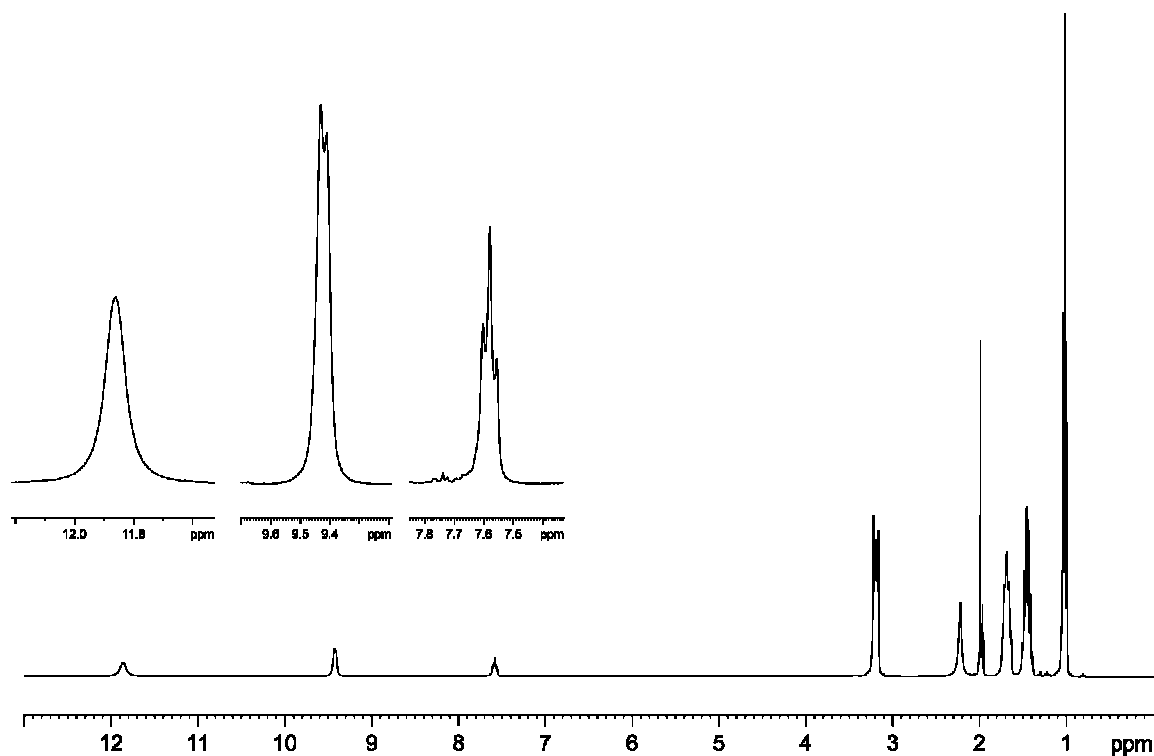


Figure 11: ^1H NMR spectrum of $\text{TBA}_3[\text{PW}_{11}\text{O}_{39}\{\text{RuNPPH}_3\}]$ (**2**)

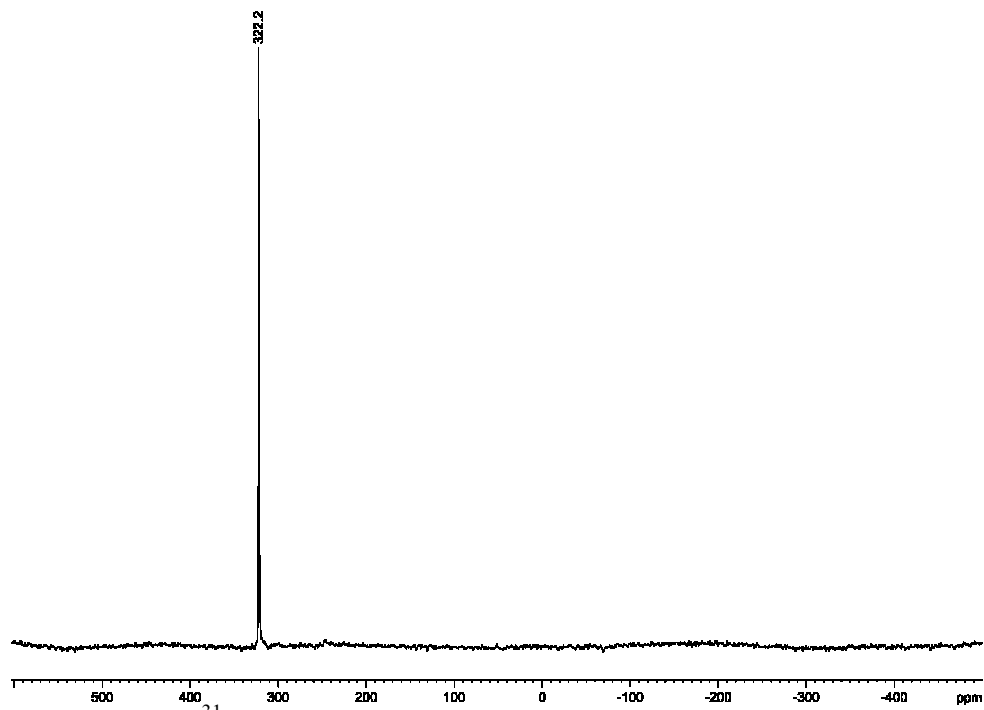


Figure 12: ^{31}P NMR spectrum of of $\text{TBA}_3[\text{PW}_{11}\text{O}_{39}\{\text{RuNPPH}_3\}]$ (2)

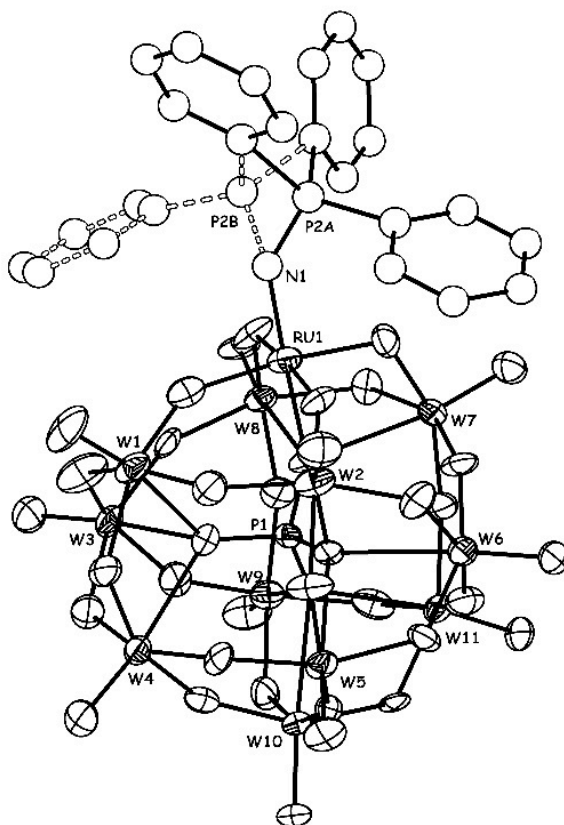
X-ray structure analysis of (TBA)₃[PW₁₁O₃₉{RuN(C₆H₅)₃}] (2)

Diffraction data of **2** were collected, using a combination of φ and ω scans, on a Nonius Kappa-CCD diffractometer (Table 1) with graphite monochromated Mo-K α (0.71073 Å) radiation. Measurements were performed at 200 K, because of the poor stability of the crystals at room temperature. Even sealed in a Lindeman tube in the presence of the mother liquor, the crystal showed some decay. Unit cell parameters determination, data collection strategy and integration were carried out with the Nonius Eval-14 suite of programs.² The data were corrected from absorption by a multiscan method.³ The structure was solved by direct methods with SHELXS-86,⁴ refined by full least-squares on F^2 and completed with SHELXL-97.⁵ Graphics were carried out with DIAMOND.⁶ The hydrogen atoms have not been introduced in the model. Only the tungsten, ruthenium, oxygen atoms and the phosphorous atom belonging to the phosphate group have been anisotropically refined. The phosphorus atom of the phosphoraniminato ligand showed some disorder between two positions, P2A and P2B accounting each for an occupation ratio of one half. Similarly one of the phenyl ring is disordered between two equivalent sites (C62A to C67A and C62B to C67B, each with an occupancy of one half). The three phenyl groups have been restrained and refined as rigid groups with C-C distances set to 1.39 Å and CCC angles to 120°. Due to the high disorder affecting the tetrabutylammonium cations, the N-C and C-C bond lengths were also restrained to 1.55 and 1.50 Å respectively, whereas all bond angles were restrained to a value of 109°. The residual electron density is located in the vicinity of W atoms.

Empirical Formula	C ₆₆ H ₁₂₃ N ₄ P ₂ W ₁₁ Ru ₁ O ₃₉
M_r	3782.08
Color	Orange
Temperature /K	250
Crystal System	orthorhombic
Space Group	$Pc2_1n$
a /Å	18.187(2)
b /Å	18.201(18)

$c / \text{\AA}$	34.565(5)
$\alpha / ^\circ$	90
$\beta / ^\circ$	90
$\gamma / ^\circ$	90
$V / \text{\AA}^3$	11442(2)
Z	4
$\rho_{\text{calcd}} / \text{g}\cdot\text{cm}^{-3}$	2.124
μ / cm^{-1}	1.122
$\theta_{\text{min}}-\theta_{\text{max}} / ^\circ$	2.3 – 27.5
octants colld	-23 +23, -21 23, -43 44
reflens measd	54621
unique reflens	23557
obsd reflens ($I > 2\sigma(I)$)	13920
Flack parameter	0.045(11)
refined param	733
$R_{(\text{int})}$	0.0592
R	0.0554
R_w (all data)	0.1536
goodness of fit S	0.995
$\Delta\rho(\text{max/min}) / \text{e}\cdot\text{\AA}^{-3}$	-2.388 / 2.346

The anion of **2** displays a phosphoraniminato ligand linked to the ruthenium center. Despite the encountered disorder, the geometrical parameters around N1 and the phosphorous atoms P2A and P2B are similar to those described in the literature for osmium-phosphoraniminato function.⁷ Structural characterisation of analogous ruthenium complexes are indeed unprecedented. The Ru1-N1 bond length of 1.923(16) Å, considerably elongated by comparison with a ruthenium-nitrido function, is nevertheless indicative of a multiple bonding. The N1-P2A or N1-P2B distances of 1.487(18) and 1.511(18) Å are a bit shorter than those reported in osmium-phosphoraniminato complexes that fall in the range 1.59-1.66 Å.⁷ The M-N-P link, which can be either linear or bent is clearly bent here with P2A-N1-Ru1 and P2B-N1-Ru1 angles respectively of 137.1 (11) and 139.1(11)°.



1

Figure 13: Representation of **2** together with the labelling scheme (Thermal ellipsoids 50%) Selected bond distances (Å) and angles (deg). Ru1-N1, 1.923(16); Ru1-O26, 1.954(13); Ru1-O39, 1.964(13); Ru1-O28, 1.963(12); Ru1-O31 1.967(13), Ru1-O33 2.200(11); P2A-N1, 1.487(18); P2A-C62A, 1.80(3); P2A-C56, 1.932(18); P2A-C50, 1.919(18); P2B-N1, 1.511(18) P2B-C62B 1.85(3); P2B-C50 1.931(19); P2B-C56 1.907(19); P2A-N1-P2B, 53.5(8); P2A-N1-Ru1, 137.1(11); P2B-N1-Ru1, 139.1(11).

References

1. Artero, V.; Laurencin, D.; Villanneau, R.; Thouvenot, R.; Herson, P.; Gouzerh, P.; Proust, A. *Inorganic Chemistry* **2005**, *44*, 2826-2835.
2. Duisenberg, A. J. M.; Kroon-Batenburg, L. M. J.; Schreurs, A. M. M., *J. Appl. Crystallogr.* **2003**, *36*, 220.
3. Blessing, R. H., *Acta Cryst.* **1995**, *A51*, 33.
4. Sheldrick, G. M., SHELX86, *Computer Program for Structure Solution*; University of Göttingen: Germany. **1986**.
5. Sheldrick, G. M., SHELX97, *Computer Program for Structure Refinement*; of Göttingen: Germany. **1997**.
6. Brandenburg, K.; Berndt, M., *Diamond*; Crystal Impact GbR: Bonn, Germany. **1999**.
7. Demadis, K. D.; Bakir, M.; Kleszczewski, B. G.; Williams, D. S.; White, P. S.; Meyer, T. J., *Inorg. Chim. Acta* **1998**, *270*, 511-526.